



**HAL**  
open science

## **Endothelial Epas1 Deficiency Is Sufficient To Promote Parietal Epithelial Cell Activation and FSGS in Experimental Hypertension**

Yosu Luque, Olivia Lenoir, Philippe Bonnin, Lise Hardy, Anna Chipont, Sandrine Placier, Sophie Vandermeersch, Yi-Chun Xu-Dubois, Blaise Robin, H el ene Lazareth, et al.

► **To cite this version:**

Yosu Luque, Olivia Lenoir, Philippe Bonnin, Lise Hardy, Anna Chipont, et al.. Endothelial Epas1 Deficiency Is Sufficient To Promote Parietal Epithelial Cell Activation and FSGS in Experimental Hypertension. *Journal of the American Society of Nephrology*, 2017, 28 (12), pp.3563-3578. 10.1681/ASN.2016090960 . hal-01713482

**HAL Id: hal-01713482**

**<https://hal.science/hal-01713482>**

Submitted on 20 Feb 2018

**HAL** is a multi-disciplinary open access archive for the deposit and dissemination of scientific research documents, whether they are published or not. The documents may come from teaching and research institutions in France or abroad, or from public or private research centers.

L'archive ouverte pluridisciplinaire **HAL**, est destin ee au d ep ot et  a la diffusion de documents scientifiques de niveau recherche, publi es ou non,  emanant des  tablissements d'enseignement et de recherche fran ais ou  trangers, des laboratoires publics ou priv es.

# Endothelial *Epas1* Deficiency Is Sufficient To Promote Parietal Epithelial Cell Activation and FSGS in Experimental Hypertension

Yosu Luque,<sup>\*†‡</sup> Olivia Lenoir,<sup>§||</sup> Philippe Bonnin,<sup>¶\*\*</sup> Lise Hardy,<sup>†</sup> Anna Chipont,<sup>§||</sup> Sandrine Placier,<sup>†</sup> Sophie Vandermeersch,<sup>†</sup> Yi-Chun Xu-Dubois,<sup>\*†</sup> Blaise Robin,<sup>§||</sup> Hélène Lazareth,<sup>§||</sup> Michèle Souyri,<sup>††‡‡</sup> Léa Guyonnet,<sup>§§</sup> Véronique Baudrie,<sup>§</sup> Eric Camerer,<sup>§||</sup> Eric Rondeau,<sup>\*†‡</sup> Laurent Mesnard,<sup>\*†‡</sup> and Pierre-Louis Tharaux<sup>§|||||</sup>

\*Critical Care Nephrology and Kidney Transplantation, Hôpital Tenon, Assistance Publique-Hôpitaux de Paris, Paris, France; †Unité Mixte de Recherche S1155, §Paris Cardiovascular Center (PARCC), \*\*Unité Mixte de Recherche 965, and ††Institut Universitaire d'Hématologie, Institut National de la Santé et de la Recherche Médicale, Paris, France; ‡University Pierre and Marie Curie, Paris, France; ¶Université Paris Descartes, Sorbonne Paris Cité, Paris, France; ¶Department of Physiology, Hôpital Lariboisière, Assistance Publique-Hôpitaux de Paris, Paris, France; ‡‡Université Paris Diderot, Sorbonne Paris Cité, Paris, France; §§National Cytometry Platform, Department of Infection and Immunity, Luxembourg Institute of Health, Esch-sur-Alzette, Luxembourg; and ||||Renal Division, Hôpital Européen Georges Pompidou, Assistance Publique-Hôpitaux de Paris, Paris, France

## ABSTRACT

FSGS, the most common primary glomerular disorder causing ESRD, is a complex disease that is only partially understood. Progressive sclerosis is a hallmark of FSGS, and genetic tracing studies have shown that parietal epithelial cells participate in the formation of sclerotic lesions. The loss of podocytes triggers a focal activation of parietal epithelial cells, which subsequently form cellular adhesions with the capillary tuft. However, in the absence of intrinsic podocyte alterations, the origin of the pathogenic signal that triggers parietal epithelial cell recruitment remains elusive. In this study, investigation of the role of the endothelial PAS domain-containing protein 1 (EPAS1), a regulatory  $\alpha$  subunit of the hypoxia-inducible factor complex, during angiotensin II–induced hypertensive nephropathy provided novel insights into FSGS pathogenesis in the absence of a primary podocyte abnormality. We infused angiotensin II into endothelial-selective *Epas1* knockout mice and their littermate controls. Although the groups presented with identical high BP, endothelial-specific *Epas1* gene deletion accentuated albuminuria with severe podocyte lesions and recruitment of pathogenic parietal glomerular epithelial cells. These lesions and dysfunction of the glomerular filtration barrier were associated with FSGS in endothelial *Epas1*-deficient mice only. These results indicate that endothelial EPAS1 has a global protective role during glomerular hypertensive injuries without influencing the hypertensive effect of angiotensin II. Furthermore, endothelial *Epas1* gene deficiency promotes FSGS in this model of hypertension, providing proof of principle that endothelial-derived signaling can trigger FSGS. These findings illustrate the potential importance of the EPAS1 endothelial transcription factor in secondary FSGS.

J Am Soc Nephrol 28: ●●–●●●, 2017. doi: <https://doi.org/10.1681/ASN.2016090960>

Hypertension is one of the most common causes of renal complications, and hypertensive nephropathy is second only to diabetes as a leading cause of progressive CKD. According to the 2011 US Renal Data System data, in the year 2009, hypertensive nephrosclerosis accounted for 28% of patients reaching ESRD. During hypertension, the role of angiotensin II (AngII) in promoting the progression of glomerular

Received September 9, 2016. Accepted June 29, 2017.

Y.L. and O.L. contributed equally to this work.

Published online ahead of print. Publication date available at [www.jasn.org](http://www.jasn.org).

**Correspondence:** Dr. Pierre-Louis Tharaux, Paris Cardiovascular Center, 56 rue Leblanc, 75015, Paris, France. Email: pierre-louis.tharaux@inserm.fr

Copyright © 2017 by the American Society of Nephrology

disease with altered glomerular filtration barrier, podocytes loss, and sclerotic scarring of glomeruli is well established.<sup>1</sup> Chronic infusion of AngII in mice provokes arterio-nephrosclerosis, with pathology in the terminal branches of the interlobular arteries, together with global glomerulosclerosis without FSGS.<sup>2–4</sup>

Glomerular hypertension results in glomerular capillary stretching, endothelial damage, and elevated glomerular protein filtration causing glomerular collapse and/or FSGS.<sup>1,5–8</sup> Moreover, the endothelium itself is a main player in the pathophysiology of hypertensive CKD<sup>9</sup> because it plays a main role in the regulation of vascular tone, inflammatory cell recruitment, delivery of oxygen, and tissue repair. During hypertension, the induction of vasoconstrictors,<sup>8</sup> increased oxygen consumption due to elevated sodium transport,<sup>10</sup> and AngII-induced oxidative stress<sup>11,12</sup> result in lower renal oxygenation,<sup>13</sup> thus suggesting that the hypoxia-inducible factor (HIF) pathway could play a role in nephropathy.

Furthermore, several studies correlate cortical hypoxia measured by magnetic resonance imaging<sup>14,15</sup> and activation of hypoxia-response genes with CKD in humans.<sup>16</sup> Loss of peritubular capillaries<sup>9</sup> and activation of hypoxic responses are common features found in many kidney diseases and in experimental models of CKD.<sup>17</sup>

HIF is a heterodimeric transcription factor composed of an oxygen-sensitive  $\alpha$  subunit and a constitutively expressed  $\beta$  subunit (also referred to as aryl hydrocarbon receptor nuclear translocator subunit).<sup>18</sup> HIF activates the transcription of a variety of genes promoting erythropoiesis, angiogenesis, glycolysis, and cell survival.<sup>19</sup> To date, three isoforms of HIF have been reported: HIF-1, HIF-2 (also known as epithelial cells and endothelial PAS domain-containing protein 1 [EPAS1]), and HIF-3. In the kidney, EPAS1 is expressed essentially in the endothelial cells, in particular in the glomerular endothelium,<sup>20,21</sup> as well as in interstitial fibroblasts and podocytes.<sup>22</sup> Increased expression of HIF-1 $\alpha$  and EPAS1 were found in both acute and chronic kidney injury.<sup>23,24</sup>

Recent studies have shown that endothelial EPAS1, and not HIF-1 $\alpha$ , confers protection during ischemic AKI and ischemia-induced oxidative stress in mice.<sup>25–27</sup> In humans, EPAS1 single nucleotide polymorphisms (SNPs) have demonstrated an association with performance-related blood parameters (*e.g.*, alterations in erythropoietin, hemoglobin, and hematocrit), adaptation to high altitude,<sup>28–31</sup> and elite endurance performance.<sup>32</sup> However, the role of EPAS1 in the pathogenesis of renal diseases has not been completely elucidated.

Here, we hypothesized that endothelial EPAS1 could drive protection against AngII-induced hypertension and glomerular injury leading to CKD. To understand the role of endothelial EPAS1 during hypertensive nephropathy, we used a genetic approach to abrogate EPAS1 expression from endothelial cells in AngII-induced hypertension in mice. We found that endothelial EPAS1 protects from glomerular injury induced by chronic hypertension. We also observed that endothelial EPAS1 abrogation aggravates podocyte and parietal epithelial

cell (PEC) injury in a BP-independent manner, and impairs renal local vasoreactivity to AngII. Our study suggests that endothelial EPAS1 dysfunction could be a susceptibility factor for hypertension-associated FSGS lesions and CKD progression.

## RESULTS

### Endothelial-Specific Deletion of *Epas1* Does Not Modify BP and Kidney Structure and Function

To determine the role of endothelial EPAS1 during hypertensive CKD, we generated endothelial-specific *Epas1* knockout mice by mating *Epas1*-floxed mice (*Epas1*<sup>lox/lox</sup>)<sup>33</sup> with mice expressing Cre recombinase under the control of the VE-cadherin promoter *Cdh5* (Figure 1A).<sup>34</sup> Characterization of *Cdh5*.Cre activity in glomerular endothelial cells *in vivo* was previously described.<sup>35</sup> By using the ROSA mt-Tomato/mt-GFP reporter strain, we confirmed a 75%–80% rate of CRE excision in the microvasculature in *Cdh5*.Cre mice (Supplemental Figure 1). RT-PCR analysis on isolated glomeruli and lung extracts from *Cdh5*.Cre-*Epas1*<sup>lox/lox</sup> mice showed a significant reduction in *Epas1* mRNA expression when compared with control animals (*Epas1*<sup>lox/lox</sup>) (Figure 1, B and C), thus demonstrating efficient endothelial *Epas1* deletion in *Cdh5*.Cre-*Epas1*<sup>lox/lox</sup> mice. Of note, other cell populations in the lungs and glomeruli may express EPAS1,<sup>36,37</sup> thus demonstrating that *Epas1* mRNA is still present in lungs and glomeruli from *Cdh5*.Cre-*Epas1*<sup>lox/lox</sup> mice. Similarly, we confirmed endothelial EPAS1 deficiency by Western blotting on isolated glomeruli (Figure 1, D and E), and by immunofluorescence analysis on kidneys (Supplemental Figure 1). *Cdh5*.Cre-*Epas1*<sup>lox/lox</sup> mice were born at a Mendelian ratio and were indiscernible from their *Epas1*<sup>lox/lox</sup> control littermates in weight and size, up to 40 weeks of age. Moreover, adult *Cdh5*.Cre-*Epas1*<sup>lox/lox</sup> mice had normal cardiac and renal function and normal BP (Figures 2, 3, and 4, A–H, Supplemental Table 1) when compared with control *Epas1*<sup>lox/lox</sup> littermates. These results show that endothelial EPAS1 is dispensable for mouse development and renal and cardiac function in the basal state.

As endothelial EPAS1 deficiency has been previously associated with altered vasoreactivity and local hypertension in the lung,<sup>38</sup> we investigated the role of endothelial EPAS1 in renal vascular response to vasoconstrictors and vasodilators. We administered an intravenous bolus of vasoconstrictors (norepinephrine and AngII) and vasodilators (acetylcholine and sodium nitroprusside) to *Cdh5*.Cre-*Epas1*<sup>lox/lox</sup> mice and their control littermates. Of note, in the basal state we did not observe any difference between *Cdh5*.Cre-*Epas1*<sup>lox/lox</sup> mice and controls in mean arterial pressure (Figure 2A), renal artery blood flow (RBF) (Figure 2C), and renal vascular resistance (RVR) (Figure 2E). Interestingly, vasoconstrictor-induced hypertension and vasodilator-induced hypotension were similar in both groups (Figure 2B). However, endothelial *Epas1* deficiency was associated with a marked decrease in renal

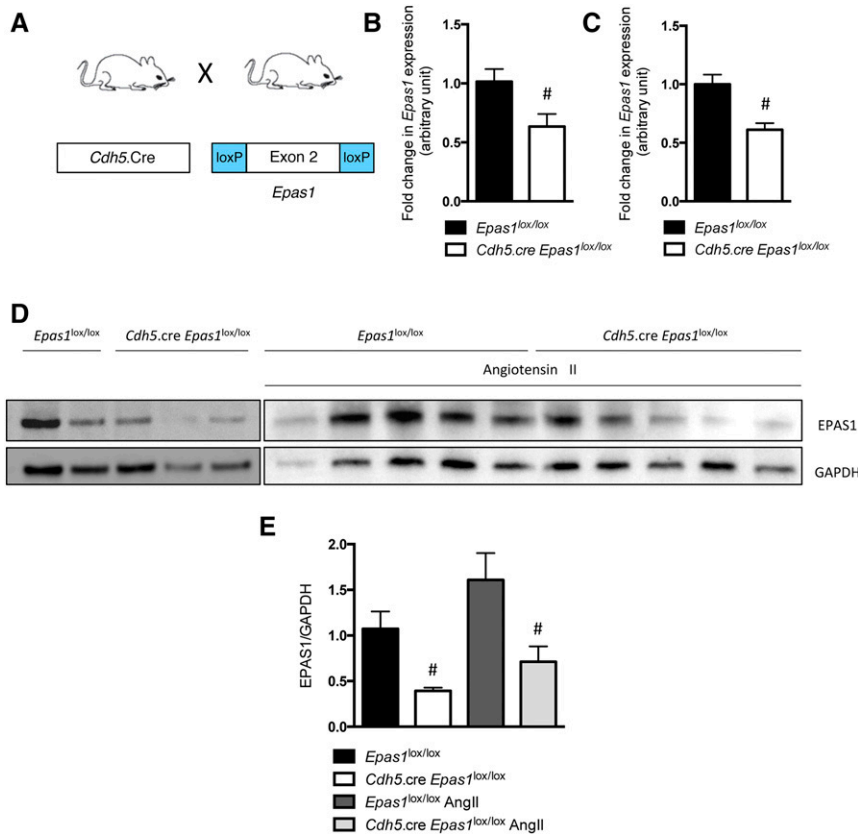


**Figure 1.** Generation of mice with a selective endothelial EPAS1 deficiency. (A) Schematic representation of the generation of mice with EPAS1-deficient endothelial cells obtained by mating mice expressing the CRE recombinase under the VE-cadherin promoter (*Cdh5.Cre* mice) with mice expressing *Epas1* alleles with loxP sites flanking exon 2 (*Epas1*<sup>lox/lox</sup> mice). (B) qPCR analysis of *Epas1* mRNA expression in glomeruli extracts from 12-week-old *Epas1*<sup>lox/lox</sup> and *Cdh5.Cre-Epas1*<sup>lox/lox</sup> mice. Data represent means±SEM of six mice. #*P*<0.05. (C) qPCR analysis of *Epas1* mRNA expression in lung extracts from 12-week-old *Epas1*<sup>lox/lox</sup> and *Cdh5.Cre-Epas1*<sup>lox/lox</sup> mice. Data represent means±SEM from six mice. #*P*<0.05. (D) Western blot analysis of EPAS1 expression in glomeruli isolated from 20-week-old *Epas1*<sup>lox/lox</sup> and *Cdh5.Cre-Epas1*<sup>lox/lox</sup> mice treated or not with AngII for 42 days. GAPDH is used as loading control. (E) Quantification of Western blot bands for EPAS1 normalized to GAPDH band intensity (means±SEM of three to six mice per group). #*P*<0.05; #different genotype, same treatment.

vascular response to AngII in *Cdh5.Cre-Epas1*<sup>lox/lox</sup> mice. Indeed, the decrease in RBF and corresponding rise in RVR elicited by acute injection of AngII were significantly attenuated in *Cdh5.Cre-Epas1*<sup>lox/lox</sup> mice (Figure 2, D and F). We observed no significant difference in renal artery vasoactivity when using norepinephrine or vasodilators, thus suggesting that endothelial *Epas1* abrogation induces a specific altered response to AngII. To confirm such an AngII-specific effect of EPAS1-mediated vasoconstriction, we evaluated the effect of the AngII receptor antagonist losartan, which normalized BP, RBF, and vascular resistance in AngII-treated *Cdh5.Cre-Epas1*<sup>lox/lox</sup> and *Epas1*<sup>lox/lox</sup> mice. Taken together, these experiments suggest that EPAS1-mediated vasoconstriction is specific to AngII (Figure 3), and that EPAS1 functionally influences the

renal endothelium in normal mice and is involved in the vasoconstriction response to AngII in the kidney.

We then examined the effect of endothelial EPAS1 deficiency during hypertension. To this end, AngII was infused in *Cdh5.Cre-Epas1*<sup>lox/lox</sup> mice and *Epas1*<sup>lox/lox</sup> control littermates for 6 weeks. Interestingly, EPAS1 expression was significantly more upregulated in glomeruli from *Epas1*<sup>lox/lox</sup> mice than those from *Cdh5.Cre-Epas1*<sup>lox/lox</sup> mice after 6 weeks of chronic AngII infusion (Figure 1, D and E), suggesting that EPAS1 is, at least partly, overexpressed by glomerular endothelial cells on hypertensive stimuli.

### Endothelial *Epas1* Gene Deletion Aggravates AngII-Induced Albuminuria in a BP-Independent Manner

In both groups, AngII infusion induced a similar gradual increase of systolic and diastolic BP (Figure 4, A and B). Importantly, heart rate, cardiac function, and cardiac parameters were similar between the two groups. Interestingly, during the first week of AngII infusion, *Cdh5.Cre-Epas1*<sup>lox/lox</sup> mice showed impaired response to AngII perfusion, as shown by a delay in hypertension development associated with lower heart rate. This difference in kinetics of hypertension induction was compensated after 7 days of AngII infusion (Figure 4, A–C). Hypertension-associated interventricular septum hypertrophy and decrease of cardiac output were observed in both groups after 6 weeks (Figure 4, C, G, and H, Supplemental Table 1). After 6 weeks of AngII infusion, when compared with hypertensive controls, the selective *Epas1* endothelial deletion was associated with a significant increase in albumin-to-creatinine ratio (Figure 4E) and kidney hypertrophy estimated by kidney-to-body weight ratio (Figure 4F), whereas the renal function, as estimated by BUN levels, was similarly altered between the two groups (Figure 4D). Interestingly, albumin-to-creatinine ratio was significantly increased in *Cdh5.Cre-Epas1*<sup>lox/lox</sup> mice as early as 7 days of AngII infusion (Supplemental Figure 2), before the development of histologic damage. Dysfunction of the glomerular filtration barrier was associated with a more profound increase in the glomerular surface in EPAS1-deficient mice (Figure 4I) with a similar nephron number (not shown) in both groups. Taken together, these results indicate that EPAS1 protects the glomerular filtration barrier integrity and may modulate glomerular capillary pressure during AngII-induced hypertension.

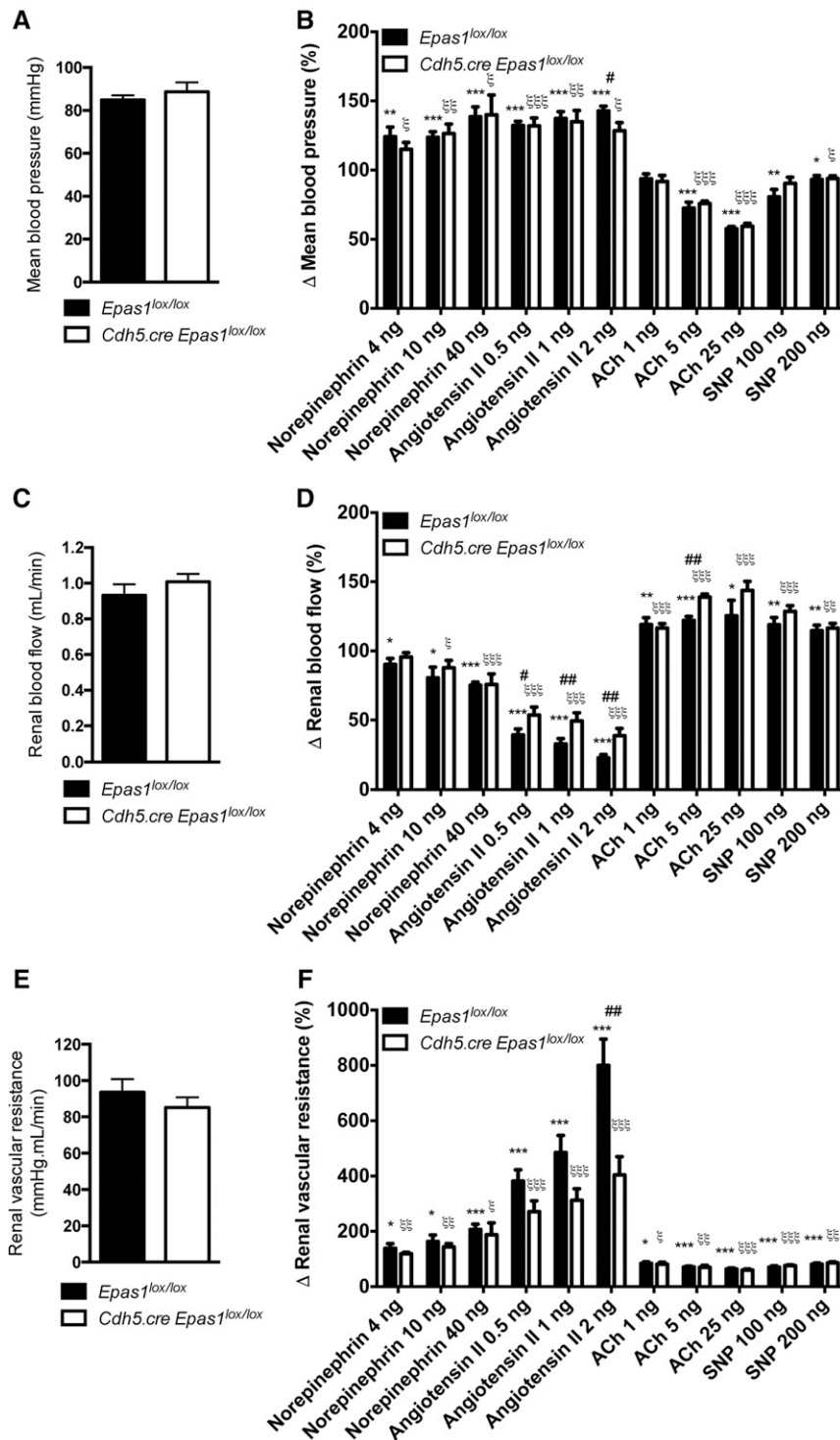


**Figure 2.** Endothelial EPAS1 deficiency is associated with a blunted renal vascular response to AngII with a similar hypertensive effect. (A) Mean arterial pressure, (C) RBF, and (E) RVR at basal state in pentobarbital-anesthetized 10- to 12-week-old *Epas1<sup>lox/lox</sup>* and *Cdh5.Cre-Epas1<sup>lox/lox</sup>* mice. Maximum changes in (B) mean arterial pressure, (D) RBF, and (F) RVR produced by 2, 4, or 10 ng norepinephrine; 0.5, 1, or 2 ng AngII; 1, 5, or 25 ng acetylcholine, or 100 or 200 ng sodium nitroprusside in 10- to 12-week-old *Epas1<sup>lox/lox</sup>* and *Cdh5.Cre-Epas1<sup>lox/lox</sup>* mice. Data represent mean  $\pm$  SEM of  $n=10-15$  mice. \**Epas1<sup>lox/lox</sup>* genotype compared with basal state; †*Cdh5.Cre-Epas1<sup>lox/lox</sup>* genotype compared with basal state; #different genotype, same treatment. \* $P<0.05$ ; \*\* $P<0.01$ ; \*\*\* $P<0.001$ .

### Deletion of *Epas1* Specifically in Endothelial Cells Favors Hypertension-Induced Glomerulosclerosis

We then performed histologic analysis of kidneys from hypertensive *Cdh5.Cre-Epas1<sup>lox/lox</sup>* mice and *Epas1<sup>lox/lox</sup>* hypertensive littermates. As expected, 6 weeks of AngII infusion revealed the presence of common hypertensive lesions in all renal compartments, such as interstitial inflammatory infiltrates (Supplemental Figure 3), glomerulosclerosis (Figure 5, A, B, and D), and tubular dilation (Figure 5F). As *Cdh5.Cre* mouse strains are known to induce off-target gene deletion in hematopoietic cells, we evaluated the effect of putative off-target *Epas1* deletion in hematopoietic cells in our model. We did not observe any change in EPAS1 expression in spleen and bone marrow-derived macrophages (BMDM) from *Cdh5.Cre-Epas1<sup>lox/lox</sup>* mice (Supplemental Figure 4). Correlating with no detectable EPAS1 deficiency in hematopoietic cells, BMDM from *Epas1<sup>lox/lox</sup>* mice and *Cdh5.Cre-Epas1<sup>lox/lox</sup>* mice similarly expressed M1/M2 differentiation markers and had a similar response to LPS stimulation (Supplemental Figure 4). Flow cytometry analysis on blood and splenic leukocytes from hypertensive *Epas1<sup>lox/lox</sup>* mice and *Cdh5.Cre-Epas1<sup>lox/lox</sup>* mice showed no difference in leukocyte populations between the two genotypes (Supplemental Figure 5). Finally, blood counts were identical in hypertensive *Epas1<sup>lox/lox</sup>* mice and *Cdh5.Cre-Epas1<sup>lox/lox</sup>* mice (Supplemental Table 2). These results support the fact that off-target *Epas1* deletion in hematopoietic cells does not occur at a detectable level in the present model.

*Cdh5.Cre-Epas1<sup>lox/lox</sup>* mice demonstrated more severe glomerular injury. Glomerular sclerotic lesions increased two- to three-fold compared with hypertensive *Epas1<sup>lox/lox</sup>* mice (Figure 5, A, B, and D). Particularly, *Cdh5.Cre-Epas1<sup>lox/lox</sup>* hypertensive mice displayed glomerular podocyte-PEC bridges and FSGS that were rarely observed in hypertensive *Epas1<sup>lox/lox</sup>* controls (Figure 5, A and B). By contrast, both hypertensive groups displayed similar interstitial fibrosis and interstitial and perivascular collagen IV deposition (Figure 5, C and E, Supplemental Figure 6). These results indicate that endothelial EPAS1 strongly influences the type of glomerular

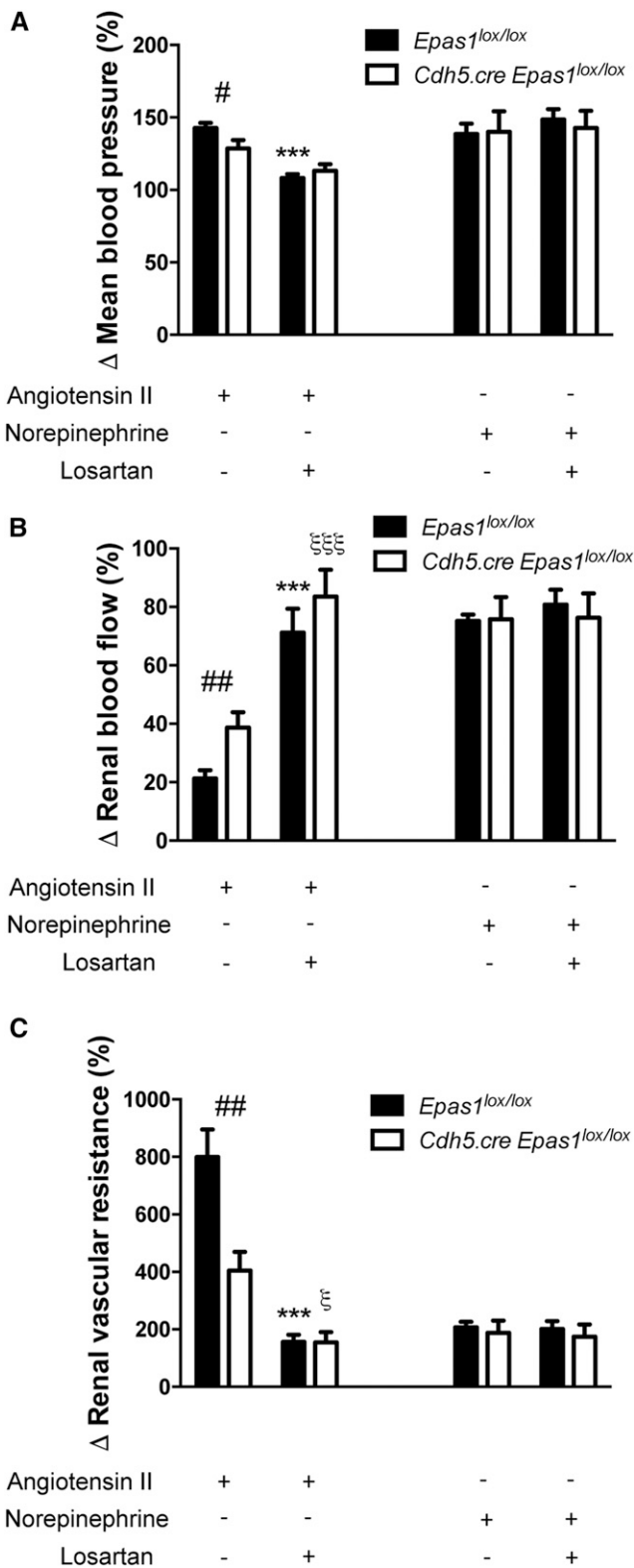


**Figure 3.** Effect of losartan on vascular resistance shows that EPAS1-induced vasoconstriction is specific to AngII. Maximum changes in (A) mean arterial pressure, (B) RBF, and (C) RVR produced by 2 ng AngII or 40 ng norepinephrine in 10- to 12-week-old *Epas1*<sup>lox/lox</sup> and *Cdh5.Cre-Epas1*<sup>lox/lox</sup> mice. Mice were pretreated with 20  $\mu$ g losartan 5 minutes

injury induced by AngII. Importantly, the increased glomerulosclerosis observed in hypertensive *Cdh5.Cre-Epas1*<sup>lox/lox</sup> mice was accompanied by an equivalent increase in renal arterial diameter and mesangial cell density than that measured in hypertensive *Epas1*<sup>lox/lox</sup> mice, as quantified by GATA3 nuclear staining (Supplemental Figures 6 and 7). Interestingly, despite similar inflammatory infiltrates and fibrosis, hypertensive *Cdh5.Cre-Epas1*<sup>lox/lox</sup> mice showed increased staining for the tubular injury marker KIM1 (Supplemental Figure 8), thus suggesting that glomerular injury mediates tubular injury.

### Endothelial EPAS1 Deficiency Promotes Hypertension-Induced Endothelial Damage

The endothelium plays a key role in the glomerular filtration barrier and endothelial intercellular junctions modulate glomerular permeability. We observed that endothelial *Epas1* abrogation was associated with decreased CD31/PECAM-1 protein expression in glomeruli (Figure 6A) from hypertensive *Cdh5.Cre-Epas1*<sup>lox/lox</sup> mice when compared with hypertensive control littermates. Furthermore, hypertension-associated capillary rarefaction in the tubular interstitium was more pronounced in *Cdh5.Cre-Epas1*<sup>lox/lox</sup> mice than in *Epas1*<sup>lox/lox</sup> mice (Figure 6, B and C). Interestingly, ultrastructural analyses revealed more severe endothelial alterations, as shown by the loss of fenestrations, cytoplasmic thickening, and vacuolization, in hypertensive *Cdh5.Cre-Epas1*<sup>lox/lox</sup> mice than in hypertensive controls (Figure 6D), confirming increased endothelial injury in glomeruli with an endothelial *Epas1* deficiency. Thus, endothelial EPAS1 promotes renal endothelial survival and maintenance during hypertensive nephropathy.

### Endothelial *Epas1* Deletion Accentuates Podocyte Dedifferentiation and Loss, Glomerular PEC Activation, and Extracellular Matrix Deposition Mimicking FSGS Lesions during AngII-Induced Hypertension

We then investigated the role of endothelial EPAS1 in podocyte and PEC structure and phenotype after AngII infusion. Immunofluorescence analysis showed that the abundance of the slit diaphragm proteins NPHS2/podocin and NPHS1/nephrin, and of PODXL/podocalyxin, were strongly reduced in glomeruli from hypertensive *Cdh5.Cre-Epas1*<sup>lox/lox</sup> mice, whereas the expression of these proteins was only slightly decreased in hypertensive control mice when compared with nonhypertensive mice (Figure 7A). WT1 immunohistochemistry demonstrated that AngII infusion induced podocyte loss to the same extent in both groups. Thus, endothelial EPAS1 deficiency

before AngII or norepinephrine treatment.  $n=5$  mice per group. Data represent mean  $\pm$  SEM. \**Epas1*<sup>lox/lox</sup> genotype AngII+losartan compared with AngII;  $\xi$ *Cdh5.Cre-Epas1*<sup>lox/lox</sup> genotype AngII+losartan compared with AngII; #different genotype, same treatment. \* $P<0.05$ ; ## $P<0.01$ ; \*\*\* $P<0.001$ .

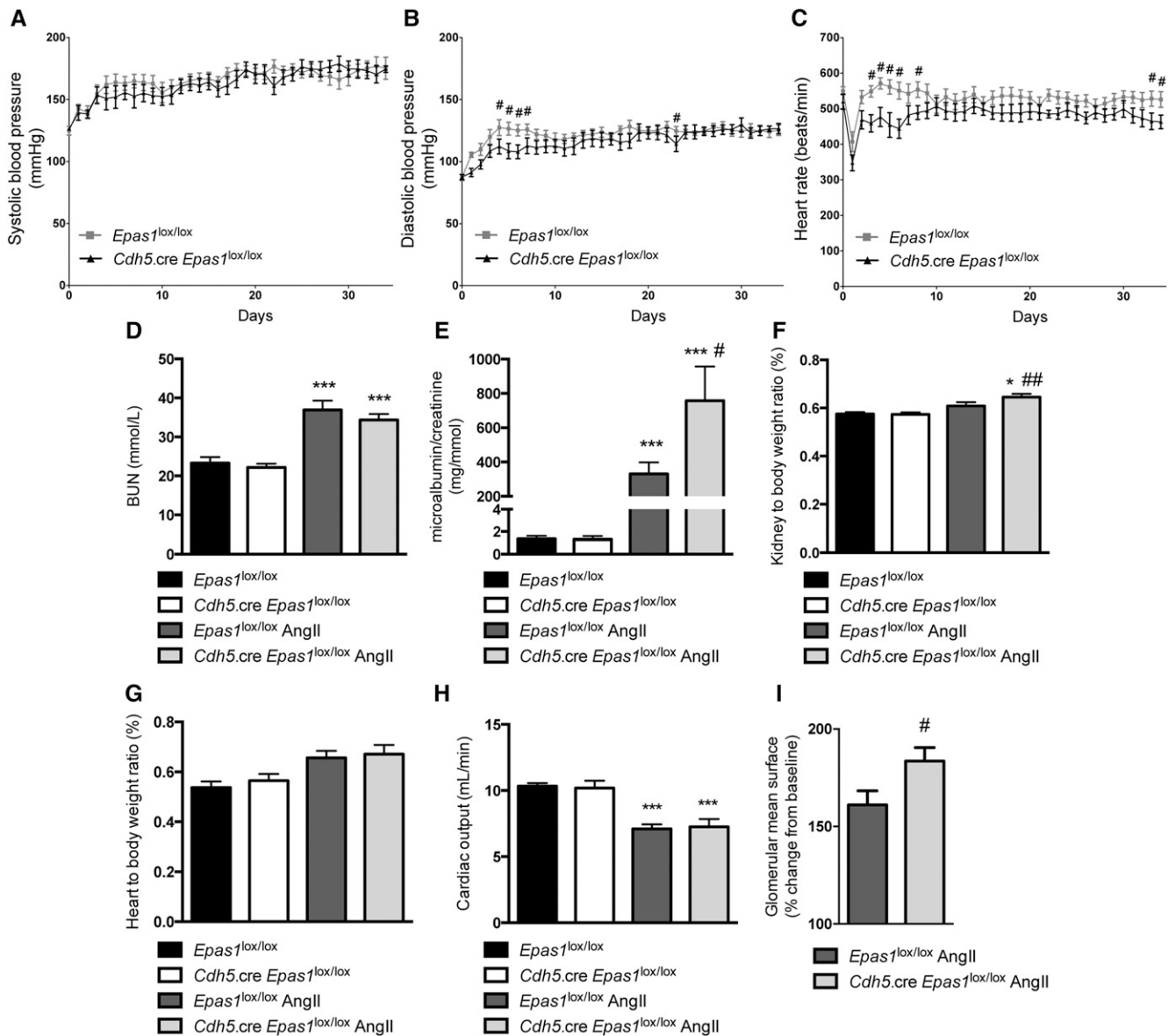


**Figure 4.** Endothelial EPAS1 deficiency aggravates AngII-induced albuminuria in a BP-independent manner. (A) Systolic BP, (B) diastolic BP, and (C) heart rate were recorded by radiotelemetry over 35 days in *Epas1*<sup>lox/lox</sup> (n=9) and *Cdh5.Cre-Epas1*<sup>lox/lox</sup> (n=7) mice at baseline and under AngII subcutaneous infusion (1 μg/kg per minute). For all panels, data correspond to the 12-hour night period. Data represent mean±SEM. #P<0.05. (D) BUN concentration, (E) urinary albumin excretion rate, and (F) kidney-to-body weight ratio in 20-week-old *Epas1*<sup>lox/lox</sup> and *Cdh5.Cre-Epas1*<sup>lox/lox</sup> mice after AngII infusion for 6 weeks in untreated *Epas1*<sup>lox/lox</sup> and *Cdh5.Cre-Epas1*<sup>lox/lox</sup> mice. (G) Cardiac output measured by noninvasive ultrasound method in *Epas1*<sup>lox/lox</sup> and *Cdh5.Cre-Epas1*<sup>lox/lox</sup> mice at baseline and after 5 weeks of AngII subcutaneous infusion. (H) Heart-to-body weight ratio and (I) glomerular mean surface variation (percentage) in kidney cortices from 20-week-old *Epas1*<sup>lox/lox</sup> and *Cdh5.Cre-Epas1*<sup>lox/lox</sup> mice after 6 weeks of AngII infusion compared with untreated *Epas1*<sup>lox/lox</sup> and *Cdh5.Cre-Epas1*<sup>lox/lox</sup> mice. Data represent mean±SEM of n=10–15 mice for (D–H), and of n=7 mice for (I). \*Same genotype, different treatment; #different genotype, same treatment. \*\*P<0.05; ##P<0.001; \*\*\*P<0.001.

promotes podocyte injury on AngII-induced hypertension (Supplemental Figure 9). Ultrastructural observations revealed more intense podocyte foot process broadening and effacement in hypertensive *Cdh5.Cre-Epas1*<sup>lox/lox</sup> glomeruli (Figure 7, B and C). *Cdh5.Cre-Epas1*<sup>lox/lox</sup> hypertensive glomeruli also displayed more glomerular podocyte–PEC bridges and FSGS than hypertensive controls (Figure 7D).

Unexpectedly, endothelial *Epas1* deletion also specifically affected glomerular PECs during hypertensive CKD. In FSGS lesions, we observed an increased activation of PECs in glomeruli from hypertensive *Cdh5.Cre-Epas1*<sup>lox/lox</sup> mice when compared with hypertensive controls, as measured by CD44 immunohistochemistry (Figure 8, A and D). CD44 expression was associated with downregulation of claudin-1 expression in

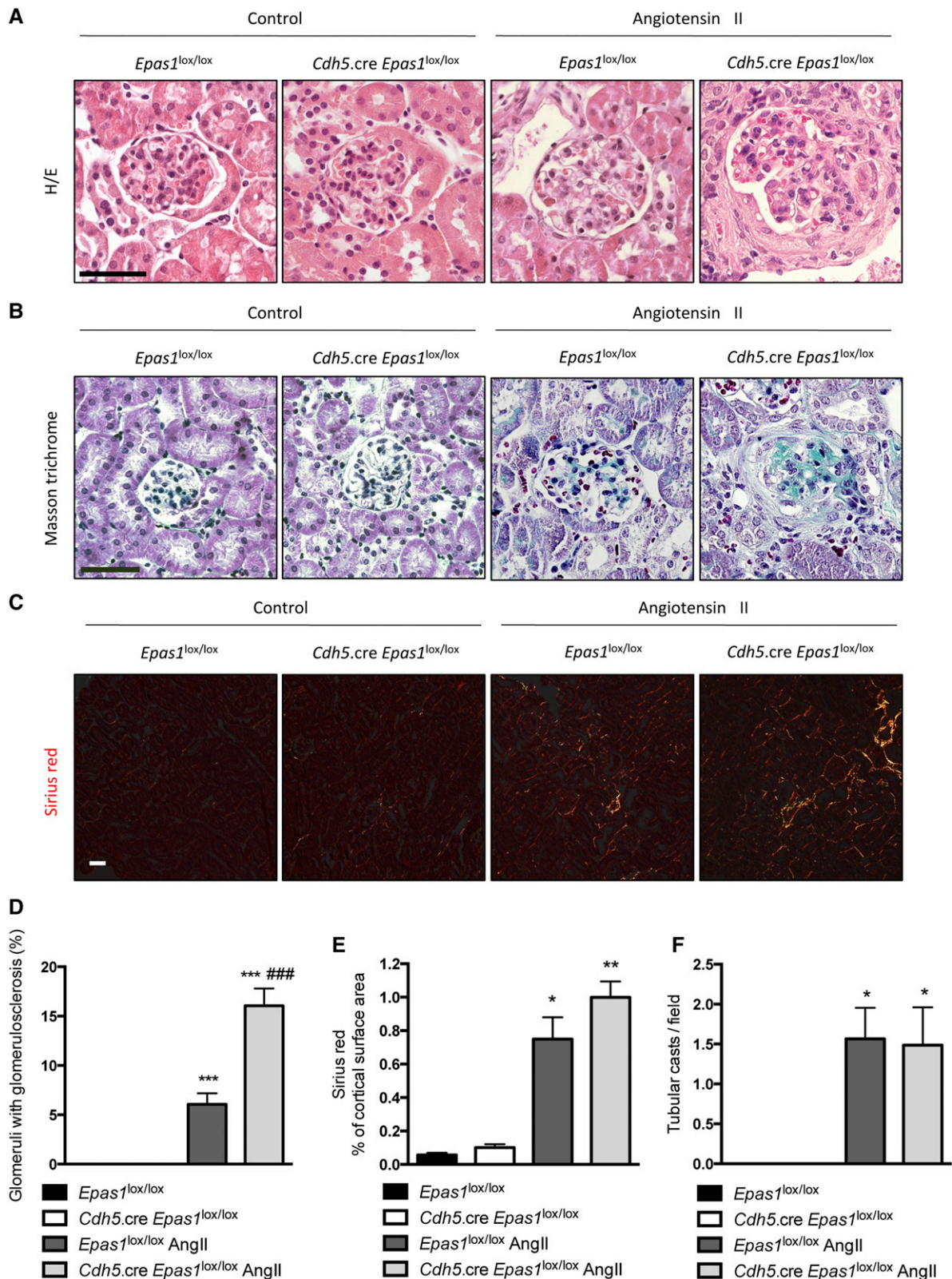


**Figure 5.** Deletion of EPAS1 specifically in endothelial cells favors hypertension-induced glomerulosclerosis. Representative images of (A) hematoxylin and eosin–stained sections, (B) Masson trichrome–stained sections, and (C) Sirius Red staining of renal cortex from 20-week-old *Epas1*<sup>lox/lox</sup> and *Cdh5.Cre-Epas1*<sup>lox/lox</sup> mice after 6 weeks of AngII infusion, and from untreated *Epas1*<sup>lox/lox</sup> and *Cdh5.Cre-Epas1*<sup>lox/lox</sup> mice. Images are representative of at least six mice per group. Scale bar, 50  $\mu$ m. (D) Quantification of the percentage of

activated PECs, which were surrounded by fibronectin deposition (Figure 8A, Supplemental Figure 10). Two distinct fibronectin deposition patterns were observed after AngII-induced hypertension. First, basal mesangial fibronectin staining was expanded after AngII infusion in every group, and that increase was more intense in *Cdh5.Cre-Epas1<sup>lox/lox</sup>* mice than in controls (Figure 8, A and B). Second, we observed a different fibronectin peripheral deposition pattern following the parietal layer of the Bowman's capsule associated with CD44 expression and FSGS lesions. This latter pattern was significantly more frequently observed in glomeruli from *Cdh5.Cre-Epas1<sup>lox/lox</sup>* hypertensive mice than in hypertensive controls (Figure 8, A–D). Altogether, these data indicate that endothelial EPAS1 deficiency exhibits global disturbance of glomerular cell homeostasis, promoting hypertension-associated secondary FSGS.

## DISCUSSION

In this study, we used a genetic approach to elucidate the role of endothelial EPAS1 during AngII-induced hypertensive nephropathy. This model shows that endothelial EPAS1 mediates glomerular protection against hypertensive injury and AngII elevated levels, with no effect observed on systemic BP. We further found that endothelium-specific EPAS1 abrogation aggravated not only hypertension-induced endothelial injury but also glomerular epithelial damage, leading to FSGS lesions.

Hypertension is the second leading cause of ESRD in the United States after diabetes and is also a consequence of CKD progression.<sup>39,40</sup> Hypertensive nephrosclerosis is a common disorder associated with hypertension and is characterized by vascular, glomerular, and tubulointerstitial lesions.<sup>41</sup> However, independent of BP levels, many studies show that individual susceptibility, such as the one conferred by *APOL1* gene variants, is involved in the diversity of observed kidney lesions. Glomerular lesions are composed of both global and FSGS.<sup>42–43</sup> Global sclerosis is thought to be related to ischemic injury, and focal lesions are classically associated with hyperfiltration from nephron loss<sup>44,45</sup> and a rise in intracapillary pressure.<sup>43–46</sup> However, local glomerular factors promoting or protecting from glomerular injury during hypertension are poorly understood. In the glomeruli, there is a close interaction between endothelial cells and epithelial cells (podocytes and parietal cells), which are separated only by the glomerular basement membrane. Hypoxia is a key mediator in CKD progression and is induced by hypertension and particularly by elevated levels of AngII.<sup>47,48</sup> However, it is likely that the glomerular endothelium is not hypoxic, and

that other pathways are involved in the constitutive endothelial EPAS1 expression.<sup>20,21</sup>

The protective role of endothelial EPAS1 during acute ischemic kidney injury has been suggested to be linked to an anti-inflammatory effect because EPAS1 deficiency was associated with increased adhesion molecule expression and leukocyte recruitment that may have occurred secondary to accentuated injury. Nevertheless, even if aggravated endothelial injury and decreased PECAM1 expression were observed in the hypertensive *Cdh5.Cre-Epas1<sup>lox/lox</sup>* mice, we did not observe any significant difference in the recruitment of macrophages and T cells or in interstitial fibrosis, suggesting a local glomerular role of endothelial EPAS1 deficiency.

Our data support a role for EPAS1 in the endothelial protection against hypertensive kidney injury. Interestingly, this protection does not act through an effect on BP. A recent study showed that endothelial EPAS1 deficiency sensitized mice to hypoxia-induced pulmonary hypertension, likely *via* increased expression of vasoconstrictor molecule endothelin-1 and a concomitant decrease in vasodilatory apelin receptor signaling.<sup>38</sup> These data may not be applicable to the renal microcirculation because we measured blunted vasoconstrictive acute response to AngII in the kidney. Moreover, telemetry measurements of BP and hemodynamic ultrasound studies showed that chronic elevation of BP and AngII-induced cardiac hypertrophy are not affected by endothelial EPAS1 deficiency.

However, peritubular capillary rarefaction is aggravated in *Epas1* knockout hypertensive mice and, consistently, RBF is diminished, indicating a crucial role of the EPAS1 pathway in the maintenance of the renal microcirculation, in glomeruli, and in the interstitium under AngII-induced stress conditions. This may be consistent with a defect of angiogenic signals produced by EPAS1/HIF-2 $\alpha$ -deficient endothelial cells in these settings. For example, Skuli *et al.*<sup>49</sup> found that hypoxic induction of the Dll4/Notch pathway target gene expression was blunted in EPAS1-deficient cultured endothelial cells.

One of the main findings of our study is that EPAS1 deficiency in endothelial cells not only accentuated glomerular injury and proteinuria but also caused a different kind of glomerular damage in hypertensive mice. FSGS is still a complex and only partially understood disease. A unifying pathophysiologic concept has not been identified and might not even exist. Elegant genetic tracing studies have shown that PECs participate in the formation of sclerotic lesions.<sup>50</sup> Here, we showed that endothelial EPAS1 response could be a key factor linking endothelial injury and epithelial glomerular cell activation. Whereas wild-type mice displayed classic angiosclerosis and glomerulosclerosis, with mesangial deposition of

sclerotic glomeruli, (E) the percentage of cortical Sirius Red staining, and (F) the tubular casts per section in renal cortex from 20-week-old *Epas1<sup>lox/lox</sup>* and *Cdh5.Cre-Epas1<sup>lox/lox</sup>* mice after 6 weeks of AngII infusion and from untreated *Epas1<sup>lox/lox</sup>* and *Cdh5.Cre-Epas1<sup>lox/lox</sup>* mice. Data represent means  $\pm$  SEM of at least six mice. \*Same genotype, different treatment; #different genotype, same treatment. \* $P < 0.05$ ; \*\* $P < 0.01$ ; ###\*\*\* $P < 0.001$ .

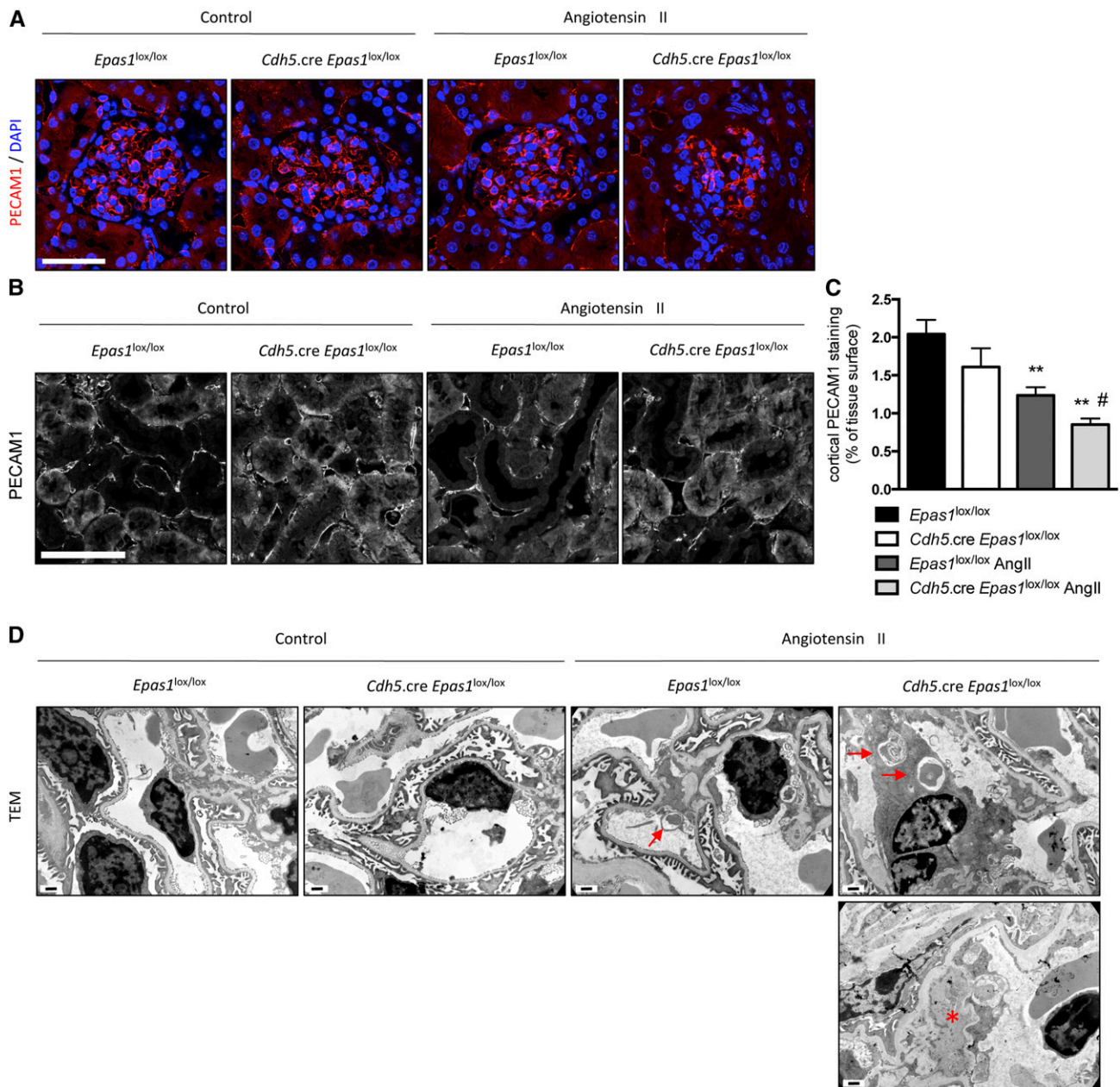


**Figure 6.** Endothelial EPAS1 deficiency promotes hypertension-induced endothelial damage. (A) Representative images of the expression of PECAM1 by immunofluorescence (red) in glomeruli and (B) renal cortices (white) in 20-week-old *Epas1*<sup>lox/lox</sup> and *Cdh5.Cre-Epas1*<sup>lox/lox</sup> mice after 6 weeks of AngII infusion and from untreated *Epas1*<sup>lox/lox</sup> and *Cdh5.Cre-Epas1*<sup>lox/lox</sup> mice. Nuclei in (A) were counterstained with DAPI stain (blue). Scale bar, 50  $\mu$ m. (C) Quantification of PECAM1 staining in renal cortex from 20-week-old *Epas1*<sup>lox/lox</sup> and *Cdh5.Cre-Epas1*<sup>lox/lox</sup> mice after 6 weeks of AngII infusion and from untreated *Epas1*<sup>lox/lox</sup> and *Cdh5.Cre-Epas1*<sup>lox/lox</sup> mice. Data represent means  $\pm$  SEM of at least five mice per group. \*Same genotype, different treatment; #different genotype, same treatment. # $P < 0.05$ ; \* $P < 0.01$ . (D) Representative photomicrographs of transmission electron microscopy sections of glomeruli from 20-week-old *Epas1*<sup>lox/lox</sup> and *Cdh5.Cre-Epas1*<sup>lox/lox</sup> mice after 6 weeks of AngII infusion and from untreated *Epas1*<sup>lox/lox</sup> and *Cdh5.Cre-Epas1*<sup>lox/lox</sup> mice showing disappearance of endothelial fenestration, subendothelial inclusions (\*), aggravated endothelial swelling, and cytoplasmic vacuolization (arrows) in endothelial cells from *Cdh5.Cre-Epas1*<sup>lox/lox</sup> mice after AngII infusion. Scale bar, 0.5  $\mu$ m. Images are representative of at least six mice.

fibronectin and few CD44-expressing PECs, endothelial-specific *Epas1* knockout mice exhibited *de novo* CD44 expression in PECs, PEC-to-glomerular tuft bridges, and extensive

fibronectin deposition in these FSGS lesions. FSGS lesions are often observed in some patients with hypertension but the mechanisms associating high BP with glomerular lesions are

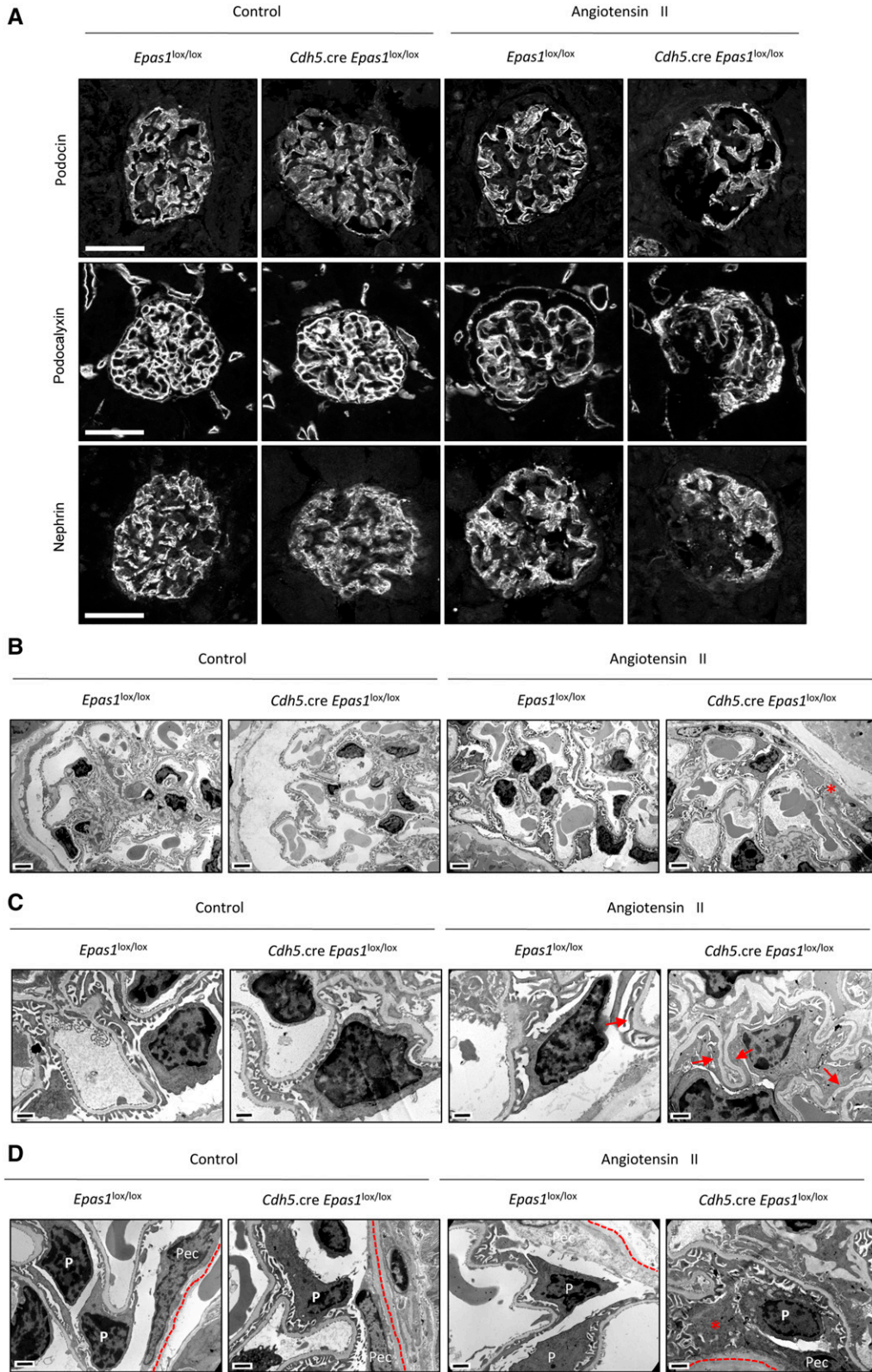


**Figure 7.** Endothelial EPAS1 deletion accelerates podocyte dedifferentiation, glomerular PEC activation, and extracellular matrix deposition mimicking FSGS lesions during AngII-induced hypertension. (A) Representative images of the expression of NPHS2/podocin (white, upper panel), PODXL/podocalyxin (white, middle panel), and NPHS1/nephrin (white, lower panel) by immunofluorescence in glomeruli from 20-week-old *Epas1<sup>lox/lox</sup>* and *Cdh5.Cre-Epas1<sup>lox/lox</sup>* mice after 6 weeks of AngII infusion and from untreated *Epas1<sup>lox/lox</sup>*

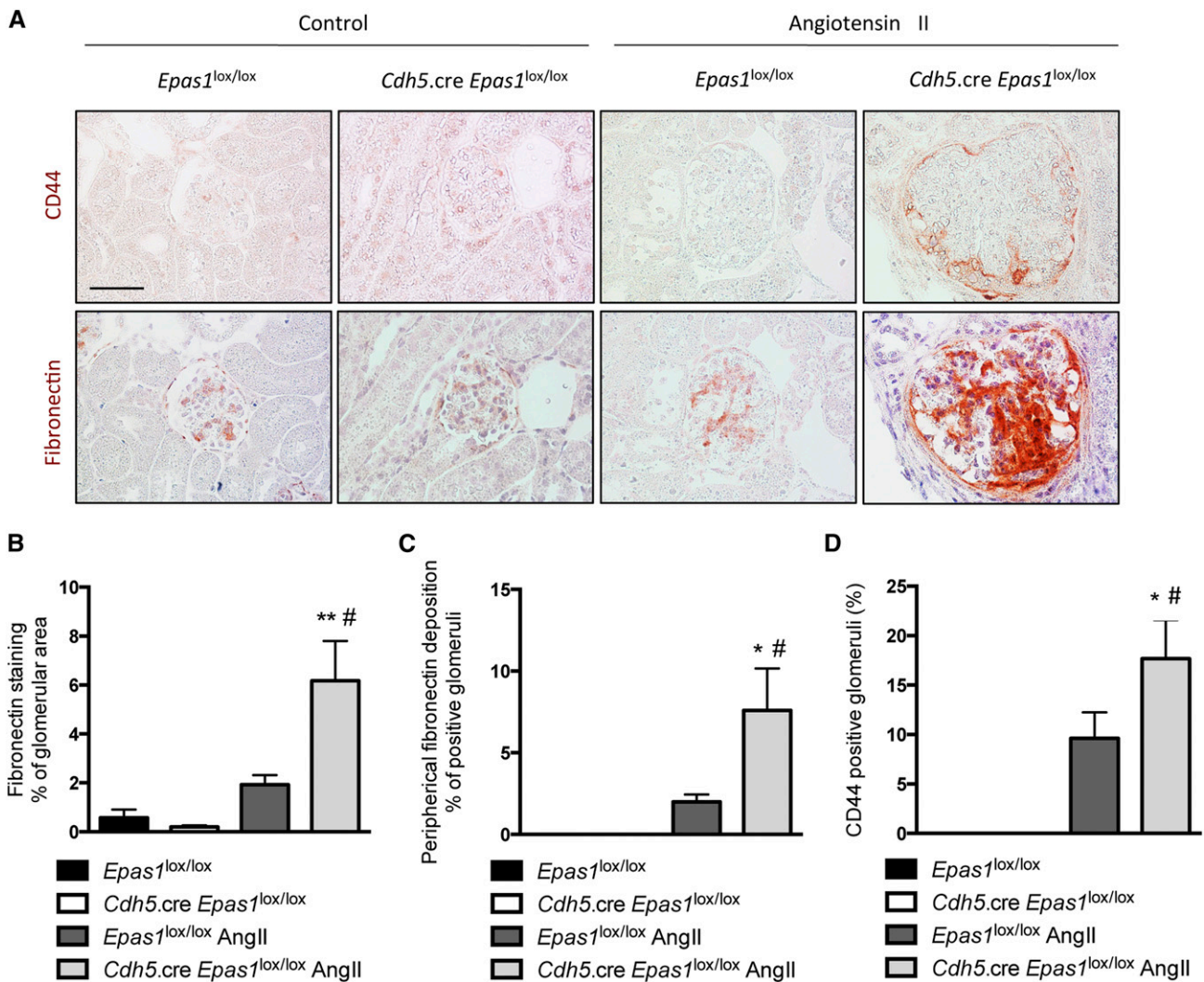


**Figure 8.** Endothelial EPAS1 deficiency promotes hypertension-induced podocyte and glomerular PEC ultrastructural alterations. (A) Representative images of CD44 (brown, upper panel), and fibronectin (brown, lower panel) expression in glomeruli from 20-week-old *Epas1*<sup>lox/lox</sup> and *Cdh5.Cre-Epas1*<sup>lox/lox</sup> mice after 6 weeks of AngII infusion and from untreated *Epas1*<sup>lox/lox</sup> and *Cdh5.Cre-Epas1*<sup>lox/lox</sup> mice showing increased PEC activation and glomerular peripheral fibronectin deposition in *Cdh5.Cre-Epas1*<sup>lox/lox</sup> AngII mice. Scale bar, 50  $\mu$ m. (B) Quantification of the percentage of fibronectin staining per glomerular area, (C) the percentage of glomeruli with peripheral fibronectin staining, and (D) the percentage of CD44-positive glomeruli in renal cortex from 20-week-old *Epas1*<sup>lox/lox</sup> and *Cdh5.Cre-Epas1*<sup>lox/lox</sup> mice after 6 weeks of AngII infusion and from untreated *Epas1*<sup>lox/lox</sup> and *Cdh5.Cre-Epas1*<sup>lox/lox</sup> mice. Data represent means  $\pm$  SEM of at least six mice. \*Same genotype, different treatment; #different genotype, same treatment. \*\* $P < 0.05$ ; \*\* $P < 0.01$ .

still elusive. The glomerular endothelial cell is not typically considered to play a major role in the development of FSGS. At early stages, even in glomeruli with extensive foot process effacement, endothelial injury is not prominent. However, at

later stages of disease, often associated with hyalinosis and sclerosis, endothelial injury becomes more obvious, but is usually considered a secondary phenomenon. The mechanisms leading to endothelial injury in FSGS are not well defined and

and *Cdh5.Cre-Epas1*<sup>lox/lox</sup> mice. (B) Representative photomicrographs of transmission electron microscopy sections of glomeruli showing cellular bridges between Bowman's capsule and glomerular tuft (\*) in *Cdh5.Cre-Epas1*<sup>lox/lox</sup> mice after 6 weeks of AngII infusion. Scale bar, 2  $\mu$ m. (C) Representative photomicrographs of transmission electron microscopy sections of glomeruli showing foot process effacement (arrows) in *Cdh5.Cre-Epas1*<sup>lox/lox</sup> mice after 6 weeks of AngII infusion. Scale bar, 0.5  $\mu$ m. (D) Representative photomicrographs of transmission electron microscopy sections of glomeruli showing cellular communication between PECs and podocytes (P) (\*) in *Cdh5.Cre-Epas1*<sup>lox/lox</sup> mice after 6 weeks of AngII infusion. Scale bar, 0.5  $\mu$ m. Images are representative of at least six mice.

endothelial-derived factors may contribute to podocyte injury. It should also be recognized that diseases that cause primary glomerular endothelium injury, such as thrombotic microangiopathy or ANCA-associated vasculitis, can lead to segmental thrombosis or glomerular injury with the development of fibrotic segmental lesions with features that fulfill the criteria for FSGS.<sup>51,52</sup> This serves to highlight that FSGS is a morphologic pattern of injury that can be derived from a diverse range of initiating insults and on different glomerular cell types.

Three main mechanistic hypotheses may explain our results. First, endothelial EPAS1 could have a direct effect on endothelial-dependent vasoreactivity and modulate glomerular pressure. Mechanical stress is believed to play a role in the progression of FSGS.<sup>53,54</sup> This hyperfiltration results in hypertrophy of glomeruli. The hypertrophy exacerbates the mismatch between the glomerular basement membrane and the decreased numbers of podocytes, resulting in further mechanical stress and injury. We have ruled out a difference in nephron number between the two groups (not shown). Interestingly, hemodynamic studies unraveled an impaired vasoconstrictive response of the renal circulation after AngII bolus injection, suggesting that endothelial EPAS1 modulates local vasoreactivity. If such altered capability to increase the RVRs affected the preglomerular circulation, one could speculate that the glomerular capillaries would then be exposed to higher hydrostatic pressure, a risk factor for podocyte mechanical stress and shedding, leading to secondary FSGS. Unfortunately, we could not measure single-nephron GFR and the glomerular capillary pressure in our mice. In fact, the kidney biopsy findings of glomerulosclerosis and larger glomerular volume were independently associated with a higher single-nephron GFR in living kidney donors,<sup>55</sup> and hypertensive *Cdh5.Cre-Epas1<sup>lox/lox</sup>* mice also displayed significantly increased glomerular area compared with controls, which supports a difference in capillary pressure. Likewise, this hypothesis may be consistent with the significant early increase in albuminuria in the *Cdh5.Cre-Epas1<sup>lox/lox</sup>* group at day 7 after AngII infusion, before the development of histopathologic damage.

Endothelial EPAS1 deficiency may also impair defense against AngII-induced endothelial dysfunction, promoting loss of endothelial permselectivity and dysfunction of the glomerular filtration barrier. Likewise, endothelial EPAS1 has been previously associated with intercellular junction integrity<sup>56</sup> and vascular permeability<sup>57</sup> in the lung. In fact, EPAS1 deficiency accentuated AngII-induced capillary rarefaction not only in glomeruli but also in the interstitium of the kidney cortex. This finding suggests that EPAS1-driven control of interstitial changes in the renal specimen may have contributed to progression of global kidney disease in addition to glomerular features. Finally, we cannot exclude that EPAS1 abrogation-induced endothelial dysfunction may influence secretion of endothelial-secreted factors acting on epithelial glomerular cells, causing podocyte injury and recruitment of pathogenic fibrogenic PECs.

Whereas gain-of-function mutations in EPAS1 are associated with paragangliomas and pheochromocytomas,<sup>58</sup> several genetic polymorphisms in *EPAS1* and its negative regulator *EGLN1*, leading to downregulation of EPAS1, were described in Tibetan native highlanders, conferring adaptation to high altitude. Indeed, a gain-of-function haplotype of *EGLN1*, conferring lower levels of EPAS1, ten specific SNP haplotypes of *EPAS1*, and a 3.4-kb copy number deletion near *EPAS1*, was found to be significantly enriched in high-altitude Tibetans and correlated with lowered hemoglobin in this population, thus allowing adaptation to high altitude-associated hypoxia.<sup>59–62</sup> *EPAS1* SNPs were also associated with elite endurance performance.<sup>63</sup> If no direct evidence associates EPAS1 downregulation with renal disease in humans, it is interesting to note the extremely high prevalence of CKD in the population of Tibet,<sup>64</sup> although specific factors linked to high-altitude adaptation, such as hyperuricemia and high hematocrit, are likely to be involved. Consequently, it would be of interest to study if a correlation exists between *EPAS1* and *EGLN1* SNP haplotypes and CKD in these two specific populations. Also, modulation of the EPAS1 cascade by yet to be identified, connected pathways may play adaptive roles in the kidney microcirculation.

In conclusion, the murine AngII-induced hypertension model developed in this study revealed a protective role of endothelial EPAS1 maintaining glomerular integrity during the hypertensive chronic insult. Interestingly, endothelial *Epas1* gene deficiency promoted podocyte damage and PEC activation and segmental sclerosis, supporting proof of principle that endothelial-derived signaling can trigger FSGS. This also suggests that endothelial EPAS1 dysfunction may be a susceptibility factor for hypertension-associated FSGS lesions and CKD progression, with endothelial *Epas1* functional variants or interacting pathways being potential key modifiers to understanding secondary FSGS lesions.

## CONCISE METHODS

### Animals

Mice with an endothelial-specific disruption of the *Epas1* gene (*Cdh5.Cre-Epas1<sup>lox/lox</sup>*) were generated by crossing *Cdh5.Cre* mice<sup>34</sup> with *Epas1<sup>lox/lox</sup>* mice.<sup>33</sup> Mice were bred on C57Bl/6J genetic background. Littermate *Epas1<sup>lox/lox</sup>* mice with no *Cre* gene were used as controls in all studies. Characterization of *Cdh5.Cre* activity in glomerular endothelial cells *in vivo* was previously described, showing a Cre efficiency of around 70% in endothelial microvascular cells.<sup>35</sup> Experiments were conducted according to the French veterinary guidelines and those formulated by the European Community for experimental animal use (L358–86/609EEC), and were approved by the Institut National de la Santé et de la Recherche Médicale and local University Research Ethics Committee (file 12–62, Comité d’Ethique en matière d’Expérimentation Animale, Paris Descartes). Mice were submitted to sanitary control tests to ensure proper pathogen-free status and were housed in the same animal facility before any experiments.

## AngII-Induced Hypertension

The hypertensive model was induced by subcutaneous infusion of AngII (Sigma-Aldrich) at a dosage of 1  $\mu\text{g}/\text{kg}$  per minute for 42 days, *via* osmotic minipumps (Model 2006; Alzet Corp.) in 12- to 14-week-old males. Pumps were implanted subcutaneously on the back between the shoulder blades and hips. Control mice were sham operated. Mice received salt supplementation (3%) in food and were euthanized 6 weeks after implantation of minipumps.

## Telemetry BP Measurement

Mice were anesthetized with isoflurane and a BP telemeter (model TA11PA-C10; Data Sciences International) was implanted in the left femoral artery. A single dose of amoxicillin (20 mg/kg administered intraperitoneally, Clamoxyl; SmithKlineBeecham) and ketoprofen (5 mg/kg administered intraperitoneally, Profenid; Aventis) was administered after the surgery. Mice were adapted for 1 week, and BP values from the last 3 days of the adaptation period were averaged to define the basal BP. On the morning of day 1, AngII-filled osmotic minipumps (Alzet Corp.) were implanted subcutaneously, as described.

## Assessment of Renal Function and Albuminuria

BUN concentrations were quantified spectrophotometrically by colorimetric methods. Urinary albumin excretion was measured with a specific ELISA assay (BIOTREND Chemikalien GmbH). Concentrations of plasma and urine electrolytes, urea and creatinine were determined with an AU 400 Chemistry Analyzer (OLYMPUS, Rungis, France).

## Histopathology and Immunohistochemistry

Kidneys were immersed in 10% formalin and embedded in paraffin. Sections (4- $\mu\text{m}$  thick) were processed for histopathology study or immunohistochemistry. Sections were stained with hematoxylin and eosin, Masson trichrome, or Sirius Red. For immunohistochemistry, paraffin-embedded sections were stained with the following primary antibodies: rat anti-PECAM1 (1:50; Dianova), rat anti-CD44 (1:100; Abcam), rabbit anti-CLAUDIN-1 (1:50; Abcam), rabbit anti-FIBRONECTIN (1:1000; Dako), rabbit anti-CD3 (1:200; Dako), rat anti-F4/80 (1:500; AbD Serotec), rabbit anti-COL4A (1:500; Abcam), goat anti-PODXL (1:500; R&D Systems), goat anti-NPHS2 (1:100; Santa Cruz Biotechnology), rabbit anti-WT1 (1:50; Abcam), rabbit anti-GATA3 (1:500; Abcam), goat anti-KIM1 (1:500; R&D systems), rabbit anti-EPAS1 (1:100; Abcam), and goat anti-NPHS1 (1:200; R&D Systems). CD3, F4/80, CD44, COL4A, KIM1, WT1, and FIBRONECTIN staining were revealed using Histofine reagent (Nichirei Biosciences). For immunofluorescence, the following secondary antibodies were used: rabbit anti-goat IgG AF594-conjugated antibody (1:400), donkey anti-rabbit AF594-conjugated (1:400), donkey anti-goat IgG AF488-conjugated antibody (1:400), ~~rabbit anti-vWF (1:10; Dako)~~, donkey anti-rat AF594-conjugated (1:400), and donkey anti-rat IgG AF488-conjugated antibody (1:500), all from Invitrogen. The nuclei were stained with DAPI. Photomicrographs were taken with an Axiophot Zeiss photomicroscope.

ImageJ software (National Institutes of Health) was used for assessment of capillary area, FIBRONECTIN deposition in glomeruli, KIM1 expression, WT1-positive nuclei per glomerular area, glomerular area, and Sirius Red staining.

The proportion of sclerotic glomeruli, CD44- and FIBRONECTIN-positive glomeruli, and GATA3- and WT1-positive nuclei per glomerular section was evaluated by examination of at least 50 glomeruli per cortical section for each mouse, by an examiner (Y.L.) who was blinded to the experimental conditions. Sclerotic glomeruli were defined as glomeruli with FSGS-like lesions, including podocyte-PEC bridges evaluated on kidney sections stained by Masson trichrome. The proportion of tubular casts was measured on kidney sections stained with Masson trichrome, evaluating at least five mice per condition.

Glomerular mean surface was evaluated on Masson trichrome-stained kidney sections by examination of at least 30 glomeruli per animal, for at least five different animals per condition.

## Isolation of Glomeruli

Decapsulated glomeruli were isolated as described previously.<sup>65,66</sup> Briefly, freshly isolated renal cortex was mixed and digested by collagenase I (2 mg/ml; Gibco) in RPMI 1640 (Life Technologies) for 2 minutes at 37°C, then collagenase I was inactivated with RPMI 1640 +10% FCS (Abcys). Tissues were then passed through a 70- $\mu\text{m}$  cell strainer and 40- $\mu\text{m}$  cell strainer (BD falcon) in PBS (Life Technologies)+0.5% BSA (Euromedex). Glomeruli, adherent to the 40- $\mu\text{m}$  cell strainer, were taken from the cell strainer with PBS+0.5% BSA injected under pressure, then washed twice in PBS. Isolated glomeruli were then picked up in radioimmunoprecipitation assay extraction buffer containing phosphatase and proteinase inhibitors (Roche) and frozen at  $-80^{\circ}\text{C}$  for protein extraction, or picked up in RLT extraction buffer (Qiagen) and frozen at  $-80^{\circ}\text{C}$  for total RNA extraction.

## Western Blot Analyses

Proteins were extracted in radioimmunoprecipitation assay buffer with protease and phosphatase inhibitors. Equal amounts of proteins were loaded onto SDS-PAGE NuPAGE 4/12% electrophoresis gels (Invitrogen and BioRad) under reducing conditions for separation and transferred onto poly(vinylidenedifluoride) membranes. The membranes were blocked with milk and probed with different antibodies: anti-EPAS1 (1:500; Novus Biologic), anti-IL1 $\beta$  (1:1000; Abcam), anti-phospho-NF $\kappa$ B (1:1000; Cell Signaling Technology), anti-TUBA/Tubulin (1:10,000; Abcam), and anti-GAPDH (1:50,000; Sigma-Aldrich). The membranes were then probed with horseradish peroxidase-conjugated secondary antibodies (1:5000; Amersham and Cell Signaling Technology) and the bands were detected by enhanced chemiluminescence using ECL Plus (Amersham and BioRad). A PXi (Syngen) imaging system was used to reveal bands and densitometric analysis was used for quantification.

## Quantitative RT-PCR

Total RNA extraction of mouse glomeruli and lung tissue was performed using an RNeasy Microkit (Qiagen). Total RNA extractions of BMDM were performed using Qiazol (Qiagen), according to manufacturer's recommendations. RNA reverse transcription was performed using the Quantitect Reverse Transcription kit (Qiagen) according to the manufacturer's protocol. The Maxima SYBR Green/Rox qPCR mix (Fermentas; Thermo Fisher Scientific) was used to amplify cDNA for 40 cycles on an ABI PRISM thermo cycler. The

comparative method of relative quantification ( $2^{-\Delta\Delta CT}$ ) was used to calculate the expression level of each target gene, normalized to *Ppia* for glomeruli and lungs, and *B2m* for BMDM. The oligonucleotide sequences are available upon request. The data are presented as the fold change in gene expression.

### Electron Microscopy

Small pieces of renal cortex were fixed in Trump fixative (EMS) and embedded in Araldite M (Sigma-Aldrich). Ultrathin sections were counterstained with uranyl acetate and lead citrate, and examined with a transmission electron microscope (JEM 1011; JEOL).

### Noninvasive Ultrasound Study of Cardiac and Renal Hemodynamics

Cardiac output, cardiac morphometry parameters, and renal hemodynamics at basal state and after AngII chronic infusion were obtained by noninvasive ultrasound technique as previously described.<sup>67</sup> Detailed methods are described in Supplemental Material.

### Renal Hemodynamics and Renal Vasoreactivity Experiments

Experiments were performed on 2-month-old male *Cdh5.Cre-Epas1<sup>lox/lox</sup>* and *Epas1<sup>lox/lox</sup>* mice. Animal surgery and RBF measurements were performed according to previously established methodology.<sup>68</sup> Briefly, after anesthesia by pentobarbital sodium (50–60 mg/kg body wt Nembutal, administered intraperitoneally), animals were placed on a servo-controlled table kept at 37°C. The left femoral artery was catheterized for measurement of arterial pressure, and a femoral venous catheter was used for infusion of volume replacement. Bovine serum albumin (4.75 g/dl of saline solution) was infused initially at 50  $\mu$ l/min to replace surgical losses, and then at 10  $\mu$ l/min for maintenance. Arterial pressure was measured *via* a pressure transducer (Statham P23 DB); RBF was measured by a flowmeter (0.5v probe TS420; Transonic Systems). RBF values were controlled for zero offset determined at the end of an experiment after cardiac arrest. Data were recorded, stored, and analyzed using Data Translation analog-to-digital converter and the IOX software (EMKA Technologies). RBF and BP were measured at basal state and during intravenous bolus injections of AngII (0.5, 1, and 2 ng) (Sigma-Aldrich), norepinephrine (2, 4, 10, and 40 ng) (Sigma-Aldrich), acetylcholine (1, 5, and 25 ng) (Sigma-Aldrich), and sodium nitroprusside (100 and 200 ng) (Sigma-Aldrich). Maximum changes in arterial pressure, RBF, and RVR produced by vasoconstrictors and vasodilators compared with the basal state of each mouse were recorded.

### Statistical Analyses

Data are expressed as mean  $\pm$  SEM. Statistical analyses were calculated with the Prism software (GraphPad). Comparison between two groups was performed with a two-tailed *t* test. Comparisons between multiple groups were performed with one-way ANOVA followed by Newman-Keuls test. A *P* value <0.05 was considered statistically significant.

### ACKNOWLEDGMENTS

We thank Elizabeth Huc and the ERI970 team for assistance in animal care and handling. We thank Thorsten Wiech (Department of Pathology,

University Hospital Eppendorf, Hamburg, Germany) for his very valuable assistance in attempts to obtain EPAS1 immunostaining in human kidneys. We thank Véronique Oberweiss, Annette De Rueda, Martine Autran, Bruno Pillard, and Philippe Coudol for administrative support. We also thank Alain Schmitt from Plateforme de Microscopie Electronique de l'Institut Cochin for transmission electron microscopy microphotograph acquisition. We thank Nicolas Sorhaindo (Centre d'Explorations Fonctionnelles Intégré, CEFI, IFR Xavier Bichat, Paris) for the determination of blood and urinary parameters in mice.

This study was supported by Institut National de la Santé et de la Recherche Médicale, the "VASCULOPHAGY" grant from the Fondation de France, the "SWITCHES" project of the Agence Nationale de la Recherche, and the European Research Council (ERC; grant 107037) to P.-L.T. Y.L. is a recipient of Fonds d'Etudes et de Recherche du Corps Médical (Assistance Publique des Hôpitaux de Paris, Paris, France), Société Française de Bienfaisance et d'Enseignement de San Sebastian-Donostia (Spain), and Société de Néphrologie grants. O.L. held postdoctoral fellowships from Société Francophone de Diabète and the Institut de France "Lefoulon-Delalande fellowship."

### DISCLOSURES

None.

### REFERENCES

- Huby AC, Rastaldi MP, Caron K, Smithies O, Dussaule JC, Chatziantoniou C: Restoration of podocyte structure and improvement of chronic renal disease in transgenic mice overexpressing renin. *PLoS One* 4: e6721, 2009
- Strupler M, Hernest M, Fligny C, Martin JL, Tharaux PL, Schanne-Klein MC: Second harmonic microscopy to quantify renal interstitial fibrosis and arterial remodeling. *J Biomed Opt* 13: 054041, 2008
- Crowley SD, Song YS, Sprung G, Griffiths R, Sparks M, Yan M, Burchette JL, Howell DN, Lin EE, Okeiyi B, Stegbauer J, Yang Y, Tharaux PL, Ruiz P: A role for angiotensin II type 1 receptors on bone marrow-derived cells in the pathogenesis of angiotensin II-dependent hypertension. *Hypertension* 55: 99–108, 2010
- Crowley SD, Frey CW, Gould SK, Griffiths R, Ruiz P, Burchette JL, Howell DN, Makhanova N, Yan M, Kim HS, Tharaux PL, Coffman TM: Stimulation of lymphocyte responses by angiotensin II promotes kidney injury in hypertension. *Am J Physiol Renal Physiol* 295: F515–F524, 2008
- Nijenhuis T, Sloan AJ, Hoenderop JG, Flesche J, van Goor H, Kistler AD, Bakker M, Bindels RJ, de Boer RA, Möller CC, Hamming I, Navis G, Wetzels JF, Berden JH, Reiser J, Faul C, van der Vlag J: Angiotensin II contributes to podocyte injury by increasing TRPC6 expression via an NFAT-mediated positive feedback signaling pathway. *Am J Pathol* 179: 1719–1732, 2011
- Casare FA, Thieme K, Costa-Pessoa JM, Rossoni LV, Couto GK, Fernandes FB, Casarini DE, Oliveira-Souza M: Renovascular remodeling and renal injury after extended angiotensin II infusion. *Am J Physiol Renal Physiol* 310: F1295–F1307, 2016
- Rennke HG: How does glomerular epithelial cell injury contribute to progressive glomerular damage? *Kidney Int Suppl* 45: S58–S63, 1994
- Johnson RJ, Feig DI, Nakagawa T, Sanchez-Lozada LG, Rodriguez-Turbe B: Pathogenesis of essential hypertension: Historical paradigms and modern insights. *J Hypertens* 26: 381–391, 2008

9. Kang DH, Kanellis J, Hugo C, Truong L, Anderson S, Kerjaschki D, Schreiner GF, Johnson RJ: Role of the microvascular endothelium in progressive renal disease. *J Am Soc Nephrol* 13: 806–816, 2002
10. Welch WJ, Baumgärtl H, Lübbers D, Wilcox CS: Renal oxygenation defects in the spontaneously hypertensive rat: Role of AT1 receptors. *Kidney Int* 63: 202–208, 2003
11. Welch WJ, Mendonca M, Aslam S, Wilcox CS: Roles of oxidative stress and AT1 receptors in renal hemodynamics and oxygenation in the postclipped 2K,1C kidney. *Hypertension* 41: 692–696, 2003
12. Welch WJ, Blau J, Xie H, Chabrashvili T, Wilcox CS: Angiotensin-induced defects in renal oxygenation: Role of oxidative stress. *Am J Physiol Heart Circ Physiol* 288: H22–H28, 2005
13. Adler S, Huang H: Impaired regulation of renal oxygen consumption in spontaneously hypertensive rats. *J Am Soc Nephrol* 13: 1788–1794, 2002
14. Inoue T, Kozawa E, Okada H, Inukai K, Watanabe S, Kikuta T, Watanabe Y, Takenaka T, Katayama S, Tanaka J, Suzuki H: Noninvasive evaluation of kidney hypoxia and fibrosis using magnetic resonance imaging. *J Am Soc Nephrol* 22: 1429–1434, 2011
15. Yin WJ, Liu F, Li XM, Yang L, Zhao S, Huang ZX, Huang YQ, Liu RB: Noninvasive evaluation of renal oxygenation in diabetic nephropathy by BOLD-MRI. *Eur J Radiol* 81: 1426–1431, 2012
16. Rudnicki M, Perco P, Enrich J, Eder S, Heininger D, Bernthaler A, Wiesinger M, Sarközi R, Noppert SJ, Schramek H, Mayer B, Oberbauer R, Mayer G: Hypoxia response and VEGF-A expression in human proximal tubular epithelial cells in stable and progressive renal disease. *Lab Invest* 89: 337–346, 2009
17. Eckardt KU, Bernhardt WM, Weidemann A, Warnecke C, Rosenberger C, Wiesener MS, Willam C: Role of hypoxia in the pathogenesis of renal disease. *Kidney Int Suppl* 68(99, Suppl): S46–S51, 2005
18. Gunaratnam L, Bonventre JV: HIF in kidney disease and development. *J Am Soc Nephrol* 20: 1877–1887, 2009
19. Schofield CJ, Ratcliffe PJ: Oxygen sensing by HIF hydroxylases. *Nat Rev Mol Cell Biol* 5: 343–354, 2004
20. St John PL, Abrahamson DR: LacZ transgenic mice and immunoelectron microscopy: An ultrastructural method for dual localization of beta-galactosidase and horseradish peroxidase. *J Histochem Cytochem* 55: 1207–1211, 2007
21. Steenhard BM, Isom K, Stroganova L, St John PL, Zelenchuk A, Freeburg PB, Holzman LB, Abrahamson DR: Deletion of von Hippel-Lindau in glomerular podocytes results in glomerular basement membrane thickening, ectopic subepithelial deposition of collagen alpha1alpha2alpha1(IV), expression of neuroglobin, and proteinuria. *Am J Pathol* 177: 84–96, 2010
22. Rosenberger C, Mandriota S, Jürgensen JS, Wiesener MS, Hörstrup JH, Frei U, Ratcliffe PJ, Maxwell PH, Bachmann S, Eckardt KU: Expression of hypoxia-inducible factor-1alpha and -2alpha in hypoxic and ischemic rat kidneys. *J Am Soc Nephrol* 13: 1721–1732, 2002
23. Nangaku M, Rosenberger C, Heyman SN, Eckardt KU: Regulation of hypoxia-inducible factor in kidney disease. *Clin Exp Pharmacol Physiol* 40: 148–157, 2013
24. Tanaka T, Yamaguchi J, Shoji K, Nangaku M: Anthracycline inhibits recruitment of hypoxia-inducible transcription factors and suppresses tumor cell migration and cardiac angiogenic response in the host. *J Biol Chem* 287: 34866–34882, 2012
25. Hill P, Shukla D, Tran MG, Aragonés J, Cook HT, Carmeliet P, Maxwell PH: Inhibition of hypoxia inducible factor hydroxylases protects against renal ischemia-reperfusion injury. *J Am Soc Nephrol* 19: 39–46, 2008
26. Tanaka T, Kato H, Kojima I, Ohse T, Son D, Tawakami T, Yatagawa T, Inagi R, Fujita T, Nangaku M: Hypoxia and expression of hypoxia-inducible factor in the aging kidney. *J Gerontol A Biol Sci Med Sci* 61: 795–805, 2006
27. Kapitsinou PP, Sano H, Michael M, Kobayashi H, Davidoff O, Bian A, Yao B, Zhang MZ, Harris RC, Duffy KJ, Erickson-Miller CL, Sutton TA, Haase VH: Endothelial HIF-2 mediates protection and recovery from ischemic kidney injury. *J Clin Invest* 124: 2396–2409, 2014
28. Beall CM, Cavalleri GL, Deng L, Elston RC, Gao Y, Knight J, Li C, Li JC, Liang Y, McCormack M, Montgomery HE, Pan H, Robbins PA, Shianna KV, Tam SC, Tsering N, Veeramah KR, Wang W, Wangdai P, Weale ME, Xu Y, Xu Z, Yang L, Zaman MJ, Zeng C, Zhang L, Zhang X, Zhaxi P, Zheng YT: Natural selection on EPAS1 (HIF2alpha) associated with low hemoglobin concentration in Tibetan highlanders. *Proc Natl Acad Sci U S A* 107: 11459–11464, 2010
29. Jeong C, Alkorta-Aranburu G, Basnyat B, Neupane M, Witonsky DB, Pritchard JK, Beall CM, Di Rienzo A: Admixture facilitates genetic adaptations to high altitude in Tibet. *Nat Commun* 5: 3281, 2014
30. Gale DP, Harten SK, Reid CD, Tuddenham EG, Maxwell PH: Autosomal dominant erythrocytosis and pulmonary arterial hypertension associated with an activating HIF2 alpha mutation. *Blood* 112: 919–921, 2008
31. Thompson AA, Elks PM, Marriott HM, Eamsamang S, Higgins KR, Lewis A, Williams L, Parmar S, Shaw G, McGrath EE, Formenti F, Van Eeden FJ, Kinnula VL, Pugh CW, Sabroe I, Dockrell DH, Chilvers ER, Robbins PA, Percy MJ, Simon MC, Johnson RS, Renshaw SA, Whyte MK, Walmsley SR: Hypoxia-inducible factor 2alpha regulates key neutrophil functions in humans, mice, and zebrafish. *Blood* 123: 366–376, 2014
32. Henderson J, Withford-Cave JM, Duffy DL, Cole SJ, Sawyer NA, Gulbin JP, Hahn A, Trent RJ, Yu B: The EPAS1 gene influences the aerobic-anaerobic contribution in elite endurance athletes. *Hum Genet* 118: 416–423, 2005
33. Gruber M, Hu CJ, Johnson RS, Brown EJ, Keith B, Simon MC: Acute postnatal ablation of Hif-2alpha results in anemia. *Proc Natl Acad Sci U S A* 104: 2301–2306, 2007
34. Oberlin E, El Hafny B, Petit-Cocault L, Souyri M: Definitive human and mouse hematopoiesis originates from the embryonic endothelium: A new class of HSCs based on VE-cadherin expression. *Int J Dev Biol* 54: 1165–1173, 2010
35. Lenoir O, Jasiek M, Hénique C, Guyonnet L, Hartleben B, Bork T, Chipont A, Flosseau K, Bensaada I, Schmitt A, Massé JM, Souyri M, Huber TB, Tharaux PL: Endothelial cell and podocyte autophagy synergistically protect from diabetes-induced glomerulosclerosis. *Autophagy* 11: 1130–1145, 2015
36. Ema M, Taya S, Yokotani N, Sogawa K, Matsuda Y, Fujii-Kuriyama Y: A novel bHLH-PAS factor with close sequence similarity to hypoxia-inducible factor 1alpha regulates the VEGF expression and is potentially involved in lung and vascular development. *Proceedings of the National Academy of Sciences of the United States of America*, 94: 4273–4278, 1997
37. Wiesener MS, Jurgensen JS, Rosenberger C, Scholze CK, Horstrup JH, Warnecke C, Mandriota S, Bechmann I, Frei UA, Pugh CW, Ratcliffe PJ, Bachmann S, Maxwell PH, Eckardt KU: Widespread hypoxia-inducible expression of HIF-2alpha in distinct cell populations of different organs. *FASEB journal: official publication of the Federation of American Societies for Experimental Biology*, 17: 271–273, 2003
38. Kapitsinou PP, Rajendran G, Astleford L, Michael M, Schonfeld MP, Fields T, Shay S, French JL, West J, Haase VH: The endothelial prolyl-4-hydroxylase domain 2/hypoxia-inducible factor 2 axis regulates pulmonary artery pressure in mice. *Mol Cell Biol* 36: 1584–1594, 2016
39. Foley RN, Collins AJ: End-stage renal disease in the United States: An update from the United States renal data system. *J Am Soc Nephrol* 18: 2644–2648, 2007
40. Collins AJ, Vassalotti JA, Wang C, Li S, Gilbertson DT, Liu J, Foley RN, Chen SC, Arneson TJ: Who should be targeted for CKD screening? Impact of diabetes, hypertension, and cardiovascular disease. *Am J Kidney Dis* 53[Suppl 3]: S71–S77, 2009
41. Freedman BI, Iskandar SS, Appel RG: The link between hypertension and nephrosclerosis. *Am J Kidney Dis* 25: 207–221, 1995
42. Harvey JM, Howie AJ, Lee SJ, Newbold KM, Adu D, Michael J, Beevers DG: Renal biopsy findings in hypertensive patients with proteinuria. *Lancet* 340: 1435–1436, 1992

43. Thadhani R, Pascual M, Nickleleit V, Tolckoff-Rubin N, Colvin R: Preliminary description of focal segmental glomerulosclerosis in patients with renovascular disease. *Lancet* 347: 231–233, 1996
44. Keller G, Zimmer G, Mall G, Ritz E, Amann K: Nephron number in patients with primary hypertension. *N Engl J Med* 348: 101–108, 2003
45. Marcantoni C, Fogo AB: A perspective on arterionephrosclerosis: From pathology to potential pathogenesis. *J Nephrol* 20: 518–524, 2007
46. Kriz W, Gretz N, Lemley KV: Progression of glomerular diseases: Is the podocyte the culprit? *Kidney Int* 54: 687–697, 1998
47. Neusser MA, Lindenmeyer MT, Moll AG, Segerer S, Edenhofer I, Sen K, Stiehl DP, Kretzler M, Gröne HJ, Schlöndorff D, Cohen CD: Human nephrosclerosis triggers a hypoxia-related glomerulopathy. *Am J Pathol* 176: 594–607, 2010
48. Zhu Q, Wang Z, Xia M, Li PL, Van Tassel BW, Abbate A, Dhaduk R, Li N: Silencing of hypoxia-inducible factor-1 $\alpha$  gene attenuated angiotensin II-induced renal injury in Sprague-Dawley rats. *Hypertension* 58: 657–664, 2011
49. Skuli N, Majmundar AJ, Krock BL, Mesquita RC, Mathew LK, Quinn ZL, Runge A, Liu L, Kim MN, Liang J, Schenkel S, Yodh AG, Keith B, Simon MC: Endothelial HIF-2 $\alpha$  regulates murine pathological angiogenesis and revascularization processes. *J Clin Invest* 122: 1427–1443, 2012
50. Smeets B, Kuppe C, Sicking EM, Fuss A, Jirak P, van Kuppevelt TH, Endlich K, Wetzels JF, Gröne HJ, Floege J, Moeller MJ: Parietal epithelial cells participate in the formation of sclerotic lesions in focal segmental glomerulosclerosis. *J Am Soc Nephrol* 22: 1262–1274, 2011
51. Noone DG, Twilt M, Hayes WN, Thomer PS, Benseler S, Laxer RM, Parekh RS, Hebert D: The new histopathologic classification of ANCA-associated GN and its association with renal outcomes in childhood. *Clin J Am Soc Nephrol* 9: 1684–1691, 2014
52. Jefferson JA, Shankland SJ: The pathogenesis of focal segmental glomerulosclerosis. *Adv Chronic Kidney Dis* 21: 408–416, 2014
53. Hostetter TH: Hyperfiltration and glomerulosclerosis. *Semin Nephrol* 23: 194–199, 2003
54. Nyberg E, Bohman SO, Berg U: Glomerular volume and renal function in children with different types of the nephrotic syndrome. *Pediatr Nephrol* 8: 285–289, 1994
55. Denic A, Mathew J, Lerman LO, Lieske JC, Larson JJ, Alexander MP, Poggio E, Glassock RJ, Rule AD: Single-nephron glomerular filtration rate in healthy adults. *N Engl J Med* 376: 2349–2357, 2017
56. Gong H, Rehman J, Tang H, Wary K, Mittal M, Chaturvedi P, Zhao YY, Komarova YA, Vogel SM, Malik AB: HIF2 $\alpha$  signaling inhibits adherens junctional disruption in acute lung injury. *J Clin Invest* 125: 652–664, 2015
57. Skuli N, Liu L, Runge A, Wang T, Yuan L, Patel S, Iruela-Arispe L, Simon MC, Keith B: Endothelial deletion of hypoxia-inducible factor-2 $\alpha$  (HIF-2 $\alpha$ ) alters vascular function and tumor angiogenesis. *Blood* 114: 469–477, 2009
58. Amorim-Pires D, Peixoto J, Lima J: Hypoxia pathway mutations in pheochromocytomas and paragangliomas. *Cytogenet Genome Res* 150: 227–241, 2016
59. Lou H, Lu Y, Lu D, Fu R, Wang X, Feng Q, Wu S, Yang Y, Li S, Kang L, Guan Y, Hoh BP, Chung YJ, Jin L, Su B, Xu S: A 3.4-kb copy-number deletion near EPAS1 is significantly enriched in high-altitude Tibetans but absent from the Denisovan sequence. *Am J Hum Genet* 97: 54–66, 2015
60. Tashi T, Scott Reading N, Wuren T, Zhang X, Moore LG, Hu H, Tang F, Shestakova A, Lorenzo F, Burjanivova T, Koul P, Guchhait P, Wittwer CT, Julian CG, Shah B, Huff CD, Gordeuk VR, Prchal JT, Ge R: Gain-of-function EGLN1 prolyl hydroxylase (PHD2 D4E:C127S) in combination with EPAS1 (HIF-2 $\alpha$ ) polymorphism lowers hemoglobin concentration in Tibetan highlanders. *J Mol Med (Berl)* 95: 665–670, 2017
61. Xu XH, Huang XW, Qun L, Li YN, Wang Y, Liu C, Ma Y, Liu QM, Sun K, Qian F, Jin L, Wang J: Two functional loci in the promoter of EPAS1 gene involved in high-altitude adaptation of Tibetans. *Sci Rep* 4: 7465, 2014
62. van Patot MC, Gassmann M: Hypoxia: Adapting to high altitude by mutating EPAS-1, the gene encoding HIF-2 $\alpha$ . *High Alt Med Biol* 12: 157–167, 2011
63. Voisin S, Cieszczyk P, Pushkarev VP, Dyatlov DA, Vashlyayev BF, Shumaylov VA, Maciejewska-Karlowska A, Sawczuk M, Skuza L, Jastrzebski Z, Bishop DJ, Eynon N: EPAS1 gene variants are associated with sprint/power athletic performance in two cohorts of European athletes. *BMC Genomics* 15: 382, 2014
64. Chen W, Liu Q, Wang H, Chen W, Johnson RJ, Dong X, Li H, Ba S, Tan J, Luo N, Liu T, He H, Yu X: Prevalence and risk factors of chronic kidney disease: A population study in the Tibetan population. *Nephrol Dial Transplant* 26: 1592–1599, 2011
65. Bollée G, Flamant M, Schordan S, Fligny C, Rumpel E, Milon M, Schordan E, Sabaa N, Vandermeersch S, Galaup A, Rodenas A, Casal I, Sunnarborg SW, Salant DJ, Kopp JB, Threadgill DW, Quaggin SE, Dussaule JC, Germain S, Mesnard L, Endlich K, Boucheix C, Belenfant X, Callard P, Endlich N, Tharaux PL: Epidermal growth factor receptor promotes glomerular injury and renal failure in rapidly progressive crescentic glomerulonephritis. *Nat Med* 17: 1242–1250, 2011
66. Henique C, Bollee G, Lenoir O, Dhaun N, Camus M, Chipont A, Flosseau K, Mandet C, Yamamoto M, Karras A, Thervet E, Bruneval P, Nochy D, Mesnard L, Tharaux PL: Nuclear factor erythroid 2-related factor 2 drives podocyte-specific expression of peroxisome proliferator-activated receptor  $\gamma$  essential for resistance to crescentic GN. *J Am Soc Nephrol* 27: 172–188, 2016
67. Sabaa N, de Franceschi L, Bonnin P, Castier Y, Malpeli G, Debbabi H, Galaup A, Maier-Redelsperger M, Vandermeersch S, Scarpa A, Janin A, Levy B, Girot R, Beuzard Y, Leboeuf C, Henri A, Germain S, Dussaule JC, Tharaux PL: Endothelin receptor antagonism prevents hypoxia-induced mortality and morbidity in a mouse model of sickle-cell disease. *J Clin Invest* 118: 1924–1933, 2008
68. Boulos N, Helle F, Dussaule JC, Placier S, Milliez P, Djudjaj S, Guerrot D, Joutel A, Ronco P, Boffa JJ, Chatziantoniou C: Notch3 is essential for regulation of the renal vascular tone. *Hypertension* 57: 1176–1182, 2011

This article contains supplemental material online at <http://jasn.asnjournals.org/lookup/suppl/doi:10.1681/ASN.2016090960/-/DCSupplemental>.